



|                  |  |
|------------------|--|
| Title            | Seismic response of sedimentary layers from comparison of surface and deep borehole recordings |
| Author(s)        | Yunsheng, Yao; SASATANI, Tsutomu   |
| Citation         | Journal of the Faculty of Science, Hokkaido University. Series 7, Geophysics, 11(6), 881-893   |
| Issue Date       | 2002-03-26   |
| Doc URL          | <a href="http://hdl.handle.net/2115/8867">http://hdl.handle.net/2115/8867</a>                  |
| Type             | bulletin (article)   |
| File Information | 11(6)_p881-893.pdf   |



[Instructions for use](#)

# Seismic Response of Sedimentary Layers from Comparison of Surface and Deep Borehole Recordings

Yao Yunsheng\* and Tsutomu Sasatani

*Division of Earth and Planetary Sciences, Graduate School of Science,  
Hokkaido University, Sapporo 060-0810, Japan*

(Received December 15, 2001)

## Abstract

Near-surface attenuation and site effect are investigated using strong motion accelerograms from sixteen local earthquakes recorded at the CNT borehole array (depths of 0, -10, -30, -100, and -467 m) installed in the Ashigara Valley, Odawara city. The investigation shows that accelerograms observed at the surface have peak amplitudes being 3 to 4 times larger than those at the deepest level. The S-wave spectral ratios of the surface spectra to the different recording level spectra are well analyzed.  $Q$  values for S-wave in sedimentary layers are obtained by fitting the theoretical transfer functions (1-D multiple reflection theory of SH-wave) to the observed spectral ratios. The results show that  $Q_s$  values are very low for the near surface layers, but have strong frequency dependence.

## 1. Introduction

The distortion of seismic waves, including attenuation, amplification and scattering, in the near-surface rocks or soils is commonly referred to as the site effect. As is well known, local site effects, especially in the site of a sedimentary basin, have an enormous influence on character of the ground motions. The spatial variations of ground shaking and resulting damage during recent large earthquakes (e.g., the 1985 Michoacan, Mexico; the 1989 Loma Prieta, California; the 1994 Northridge, California; the 1995 Hyogoken-nambu, Kobe; the 1999 Kocaeli, Turkey; and the 1999 Chi-chi, Taiwan) were clearly related to the underlying site conditions. Sediments strongly amplify seismic waves and also significantly prolong the duration of shaking; for example, Mexico City damage during the 1985 Michoacan earthquake (Celebi et al., 1987). However, many heavily developed regions, metropolitan regions, of the world are just on

---

\* Now at Institute of Seismology, China Seismological Bureau, Wuhan, China

alluvial-filled valleys.

The installation of seismometers at the surface and different depths of a borehole, that is, a borehole array, can be the ideal situation in estimating the seismic response of the sedimentary layers. The borehole array may clearly show direct evidence of amplification and attenuation of seismic waves, the magnitude and effect of nonlinear behavior of the soil response, effects of smooth versus discontinuous variation of material properties, and effects of water saturated versus dry soil at varying depths.

In this study we investigate near-surface attenuation and site effects of sedimentary layers using the borehole array records in the Ashigara Valley that is a small sedimentary basin (about  $4 \text{ km} \times 12 \text{ km}$ ). First, we estimate amplification of seismic waves based on peak ground accelerations at the surface and different recording levels. Next,  $Q$  values for S-wave in sedimentary layers are obtained by fitting the theoretical transfer functions to the observed S-wave spectral ratios (the surface spectra/the different recording level spectra).

## 2. Data

The CNT borehole array installed by Earthquake Research Institute, the

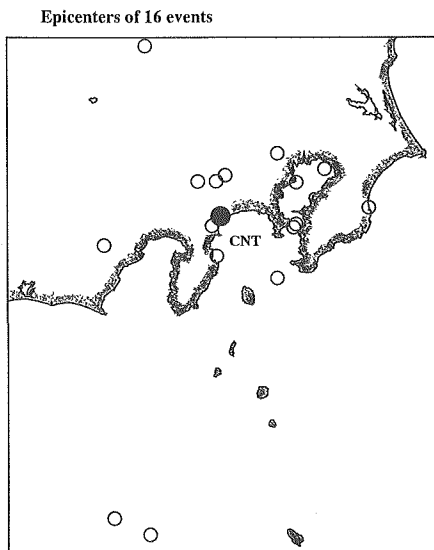


Fig. 1. Location map showing epicenters of sixteen earthquakes (open circles) used in this study and the CNT borehole array site (solid circle).

Soil profile and velocity structure of CNT borehole

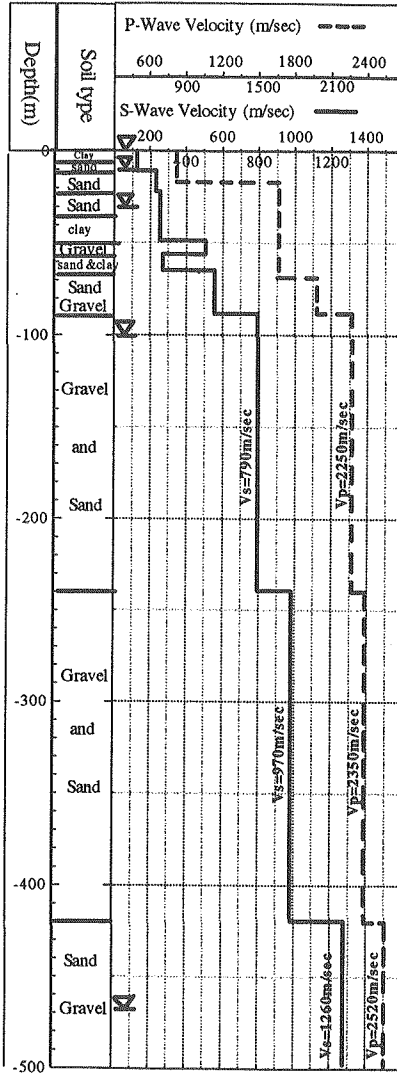


Fig. 2. Soil profile and velocity structures of the CNT borehole. Inverse triangles indicate the level of accelerometers installed.

University of Tokyo, is located in the Ashigara Valley, Odawara city, Japan (Fig. 1). This station is one of the Ashigara strong motion seismographic array that is one of ESG International Test Sites (Kudo et. al., 1988). The borehole was drilled to a depth of 500 m in Quaternary alluvium and diluvium. The Soil

Table 1. Source parameters of sixteen earthquakes used in this study.

| NO. | Origin Time<br>(Y/M/D) | Time<br>(H : M : S) | M   | Lat.<br>(°) | Long.<br>(°) | Depth<br>(km) | $\Delta$<br>(km) | Azi<br>(°) | Region           |
|-----|------------------------|---------------------|-----|-------------|--------------|---------------|------------------|------------|------------------|
| 01  | 1990/06/05/            | 22 : 42 : 53        | 5.4 | 35.553      | 139.197      | 123           | 32               | 1.0        | Central Kanagawa |
| 02  | 1990/06/27/            | 06 : 54 : 47        | 5.4 | 35.002      | 139.137      | 148           | 29               | 189.8      | Sagami Bay       |
| 03  | 1990/08/05/            | 16 : 13 : 02        | 5.1 | 35.207      | 139.095      | 14            | 10               | 212.9      | Hakone region    |
| 04  | 1990/08/23/            | 08 : 47 : 07        | 5.4 | 35.345      | 140.397      | 50            | 110              | 84.6       | Central Chiba    |
| 05  | 1990/09/24/            | 06 : 13 : 07        | 6.6 | 33.103      | 138.633      | 60            | 244              | 192.3      | Tokaido Oki      |
| 06  | 1991/04/25/            | 07 : 12 : 04        | 4.9 | 35.058      | 138.205      | 32            | 92               | 256.4      | Central Shizuoka |
| 07  | 1991/07/14/            | 23 : 19 : 10        | 5.4 | 36.417      | 138.508      | 188           | 142              | 334.6      | East Nagano      |
| 08  | 1991/11/19/            | 17 : 24 : 03        | 4.9 | 35.605      | 140.025      | 81            | 85               | 62.8       | Tokyo Bay        |
| 09  | 1992/02/02/            | 04 : 04 : 06        | 5.9 | 35.227      | 139.792      | 92            | 55               | 93.4       | Tokyo Bay        |
| 10  | 1992/04/10/            | 23 : 31 : 30        | 4.9 | 35.707      | 139.630      | 89            | 64               | 51.5       | East Tokyo       |
| 11  | 1992/05/20/            | 17 : 24 : 00        | 4.8 | 35.205      | 139.773      | 92            | 53               | 96.2       | Tokyo Bay        |
| 12  | 1992/08/30/            | 04 : 19 : 06        | 6.6 | 33.207      | 138.340      | 325           | 240              | 199.3      | Off Tokaido      |
| 13  | 1992/10/04/            | 10 : 13 : 24        | 4.6 | 34.858      | 139.640      | 31            | 60               | 137.2      | Izu Oshima       |
| 14  | 1992/10/14/            | 14 : 36 : 47        | 4.1 | 35.512      | 139.790      | 63            | 61               | 62.5       | Tokyo Bay        |
| 15  | 1992/11/08/            | 08 : 07 : 14        | 3.8 | 35.510      | 139.122      | 27            | 29               | 347.4      | Central Kanagawa |
| 16  | 1996/08/09/            | 03 : 16 : 07        | 4.4 | 35.507      | 138.971      | 21            | 34               | 324.2      | E-Yamanashi      |

$\Delta$  : epicentral distance, Azi : station-to-epicenter azimuth.

profile and velocity structures ( $V_p$  and  $V_s$ ) are shown in Fig. 2. S-wave velocity at the surface is very low ( $\sim 100$  m/s), it increases in 790 m/s at a depth of about 100 m, and reaches to 1260 m/s at a depth of 420 m. Five accelerometers were deployed at the surface (0 m) and depths of  $-10$  m,  $-30$  m,  $-100$  m and  $-467$  m. Digital data are recorded at the rate of 100 samples per second; the resolution is 18-bit words.

Calculations of the peak ground acceleration (PGA) ratio and amplitude spectral ratio between the shallow or surface recordings and the deeper ones are the most straightforward method for investigating the seismic response of sedimentary layers (amplification and attenuation). The method was used successfully by many researchers, such as Hauksson et al. (1987), Field et al., (1992), Saito et al. (1995) and Abercrombie (1997). The underlying assumption is that the deeper recording can be considered to be on the ray path between the source and the upper receiver. For this reason, we select sixteen earthquakes that occurred close to, but deeper than the borehole. The epicenters and hypocentral parameters of these events are shown in Fig. 1 and Table 1.

Figure 3 shows an example of three components of accelerograms at the different depths during the June 05, 1990 earthquake ( $M=5.4$ ). Considering the

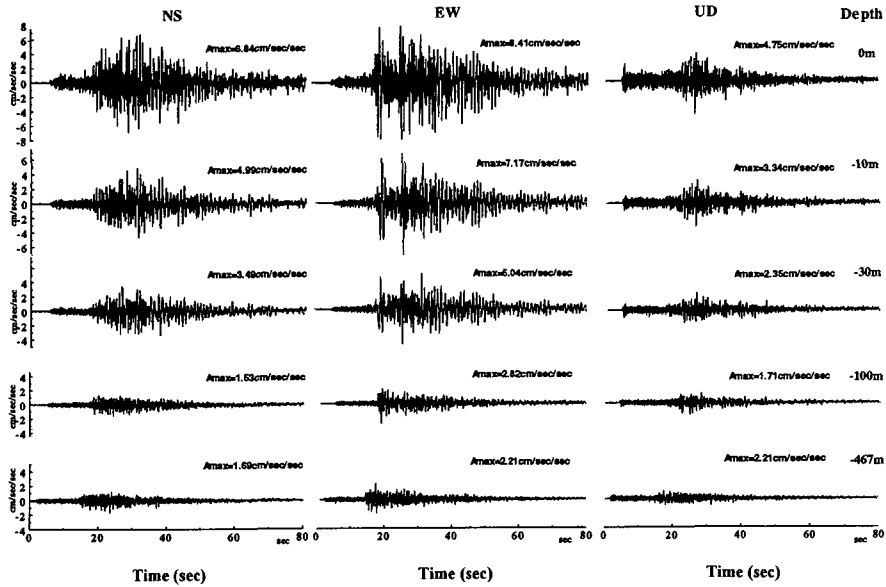


Fig. 3. An example of acceleration seismograms (three components) observed at different depths of the CNT borehole array during the June 05, 1990 event ( $M=5.4$ ).

depth of 123 km and the epicentral distance of 32 km for this event, we may assume that the seismic wave arrives at the CNT station nearly vertically. In this case, the seismogram may consist of direct P- and S-waves only. However, as shown in Fig. 3, the actual records show complex waveforms; existence of later phases of long duration. This fact indicates that the seismic response of the Ashigara Valley is not only one-dimensional but also two- and three-dimensional (Kawase and Sato, 1992; Sasatani et al., 1995). We have to take care of selecting the time window for S-wave spectral analysis as mentioned later.

### 3. Peak Ground Acceleration

The first objective of this study is to investigate peak amplitudes of the accelerograms. We can estimate the amplification of seismic motion due to resonance of near-surface layers, simply from the amplitude ratio of peak ground acceleration (PGA).

Maximum acceleration amplitude values for the sixteen events used in this study have the range of 0.34–245 cm/sec on account of their different epicentral

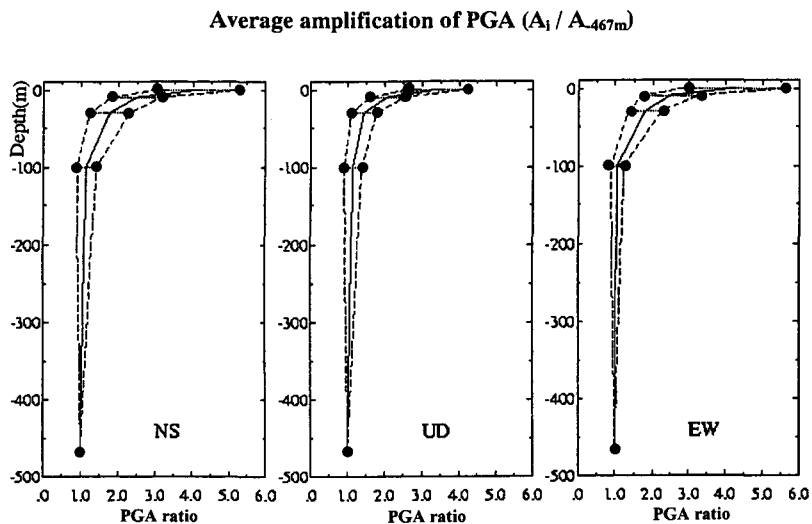


Fig. 4. Average  $A_1/A_{-467m}$  curve and its standard deviation.  $A_1$  indicates peak ground acceleration at a depth of  $i$  m.

distances, hypocentral depths and magnitudes. However, their peak amplitude ratios between the different depths and the deepest level ( $-467$  m) have a good agreement with each other. Figure 4 shows PGA amplitude ratios, the averages and their standard deviations for each component. The results show that the amplitudes of acceleration recorded at a depth of  $-100$  m are about 1.1 times as large as those recorded at a depth of  $-467$  m. However, they are amplified by about 4.2 times for NS- and EW-components, and by 3.4 times for UD-components at the surface; that is, peak ground accelerations are strongly amplified over the upper surface layers ( $\sim 100$  m). This is related to velocity change with depths as shown in Fig. 2; the velocity gradients of P- and S-waves are high over the upper surface layers ( $\sim 100$  m).

#### 4. S-wave Spectra and Their Spectral Ratios

In this section, we analyze acceleration amplitude spectra for S-waves at different depths and their spectral ratios. The S-wave spectrum is the vector sum of spectra for two horizontal components (NS and EW components). Here we assume a vertical incidence of S-wave. This assumption may be confirmed by the significant amplitudes of P-wave on the vertical component and those of S-wave on the horizontal component (see Figs. 3 and 5). All spectral analyses

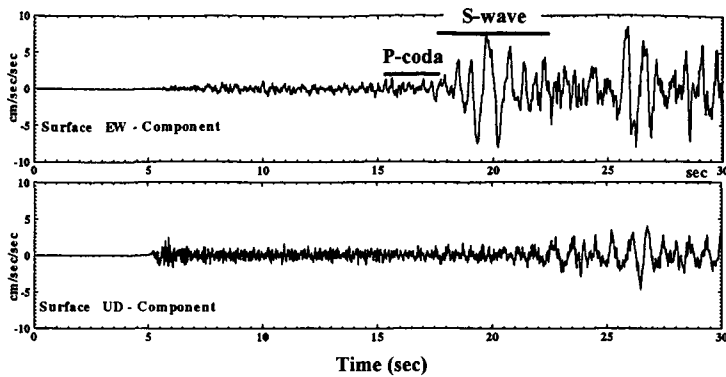


Fig. 5. Enlarged seismograms at the surface for the June 05, 1990 event ; the original ones are shown in Fig. 3. The horizontal bars indicate the time window for spectral analysis.

are done using the standard Fast Fourier Transform (FFT).

As mentioned in the previous section, the whole trace of an observed seismogram represents not only one-dimensional seismic response but also two- and three-dimensional ones. Here we are mainly concerned with one-dimensional response of S-waves. The time window selected for S-wave spectral analysis is 5.12 sec to avoid contamination of S-wave spectrum by basin surface waves that appear after the S-wave arrival as shown in Figs. 3 and 5.

For a successful spectral analysis, the data must have a good signal-to-noise ratio. We assume that the P-coda just before S-wave arrival may be included in the S-wave time window as the noise. We also calculate the P-coda spectrum (the time window of 2.56 sec) and compare it with the S-wave spectrum. In generally, S-wave spectra have much larger amplitudes than the P-coda spectra until at least 20 Hz as shown in Fig. 6.

The spectral ratios are calculated by dividing the surface spectra by those recorded at each depth for each event. Figure 7 shows original spectral ratios for sixteen events between the surface and different depths. Although the spectral shapes differ from event to event as shown in Fig. 6, the spectral ratios are nearly the same as shown in Fig. 7. Consequently we calculate the logarithmic mean values of the spectral ratios for sixteen events. Figure 8 shows the logarithmic mean values with  $\pm 1$  standard deviation. The spectral ratio shapes (e.g., peaks and troughs) considerably vary from the shallow level (0 m/–10 m) to the deep level (0 m/–467 m). The next problem is how well we can explain the shapes of spectral ratios by means of S-wave velocity ( $V_s$ ) and attenuation ( $Q_s$ ) structures.



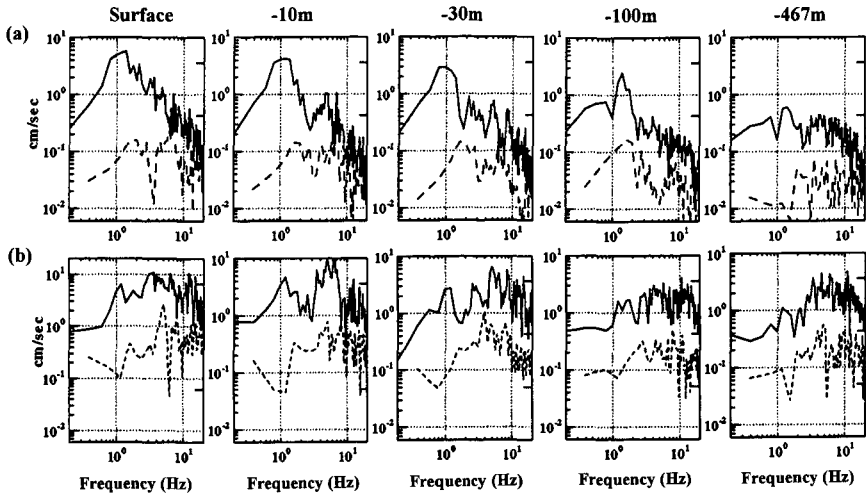


Fig. 6. Comparison between S-waves spectra (solid lines) and P-coda spectra (dashed lines) at different depths. (a): the June 05, 1990 event, and (b): the February 02, 1992 event.

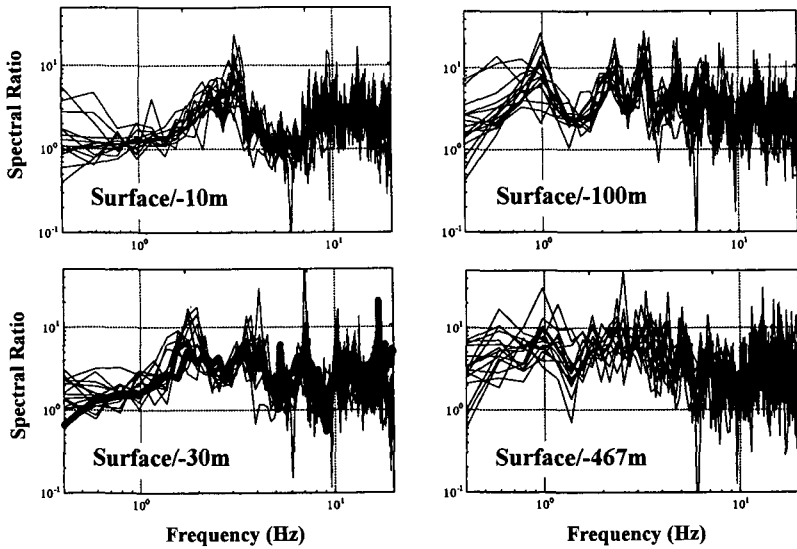


Fig. 7. S-wave spectral ratios of the surface spectra to the borehole spectra for sixteen events.

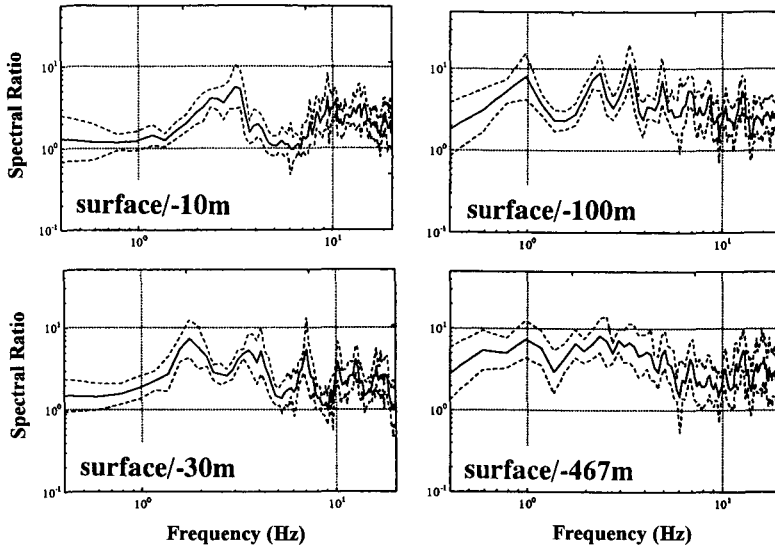


Fig. 8. Logarithmic mean values (solid lines) of S-wave spectral ratios and their standard deviations (dashed lines).

### 5. Estimation of $Q_s$ Values

In this section we try to explain the observed spectral ratios by means of  $V_s$  and  $Q_s$  structures. We fix the  $V_s$  structure model at CNT as shown in Fig. 2 and Table 4 and then we estimate  $Q_s$  structure by fitting the theoretical transfer function to the observed spectral ratio at each depth level. The theoretical transfer function is calculated by using computer program SHAKE (Schnabel et al., 1972). In this study, we assume a frequency dependent  $Q_s$  value of  $Q_s = Q_0 f^n$ ;  $Q_0$  and  $n$  are constants.

In Fig. 9, we show the method for determination of  $Q_0$  and  $n$  values. Based on the  $V_s$  structure, we calculate theoretical transfer functions for various combinations of  $Q_0$  (1.0~3.0) and  $n$  (0.0~1.0). The most plausible  $Q_0$  and  $n$  are selected for which the theoretical curve reasonably well explains the observed spectral ratio. For example, from a comparison in Fig. 9, we obtain the most plausible values of  $Q_0 = 2.0$  and  $n = 0.7$ . The  $Q_s$  values for upper layers are first estimated and then the  $Q_s$  values for lower layers are estimated by fixing the  $Q_s$  values for the upper layers.

The final  $Q_0$  and  $n$  values are also shown in Table 2. Figure 10 shows the comparison between the observed spectral ratios and estimated theoretical transfer functions at different depths. An agreement between them is generally

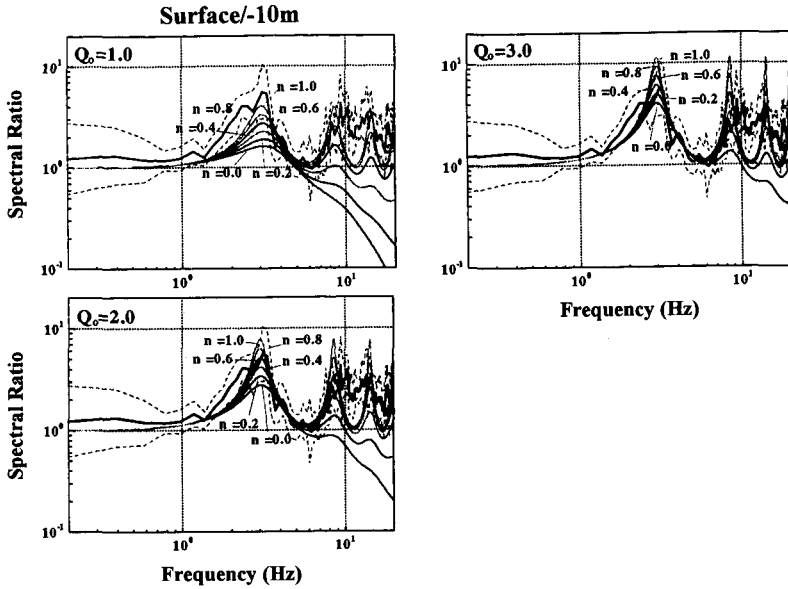


Fig. 9. Comparison between the observed spectral ratio (bold line with dashed lines as its standard deviation) and theoretical transfer functions (thin lines) for the surface/−10 m depth. The thin lines show sensitivity test of the theoretical transfer function by varying the attenuation parameters of  $Q_0$  and  $n$  ( $Q_0=1$  to 3 and  $n=0.0$  to 1.0).

Table 2. S-wave velocity structure model and  $Q_s$  values estimated in this study.

| Layer NO. | Depth m   | Thickness m | $V_s$ m/sec | $\rho$ g/cm <sup>3</sup> | $Q_s (= Q_0 f^n)$ |     |
|-----------|-----------|-------------|-------------|--------------------------|-------------------|-----|
|           |           |             |             |                          | $Q_0$             | $n$ |
| 1         | 0- 6 m    | 6           | 110         | 1.6                      | 2                 | 0.7 |
| 2         | 6- 11 m   | 5           | 120         | 1.7                      | 2                 | 0.7 |
| 3         | 11- 23 m  | 12          | 220         | 1.8                      | 3.5               | 0.9 |
| 4         | 23- 35 m  | 12          | 250         | 1.9                      | 4                 | 0.9 |
| 5         | 35- 50 m  | 15          | 250         | 1.7                      | 5                 | 0.7 |
| 6         | 50- 57 m  | 7           | 500         | 2.1                      | 9                 | 0.6 |
| 7         | 57- 68 m  | 11          | 270         | 1.8                      | 6                 | 0.6 |
| 8         | 68- 90 m  | 22          | 560         | 2.1                      | 8                 | 0.8 |
| 9         | 90-240 m  | 150         | 790         | 2.1                      | 10                | 0.6 |
| 10        | 240-420 m | 180         | 970         | 2.2                      | 10                | 0.6 |
| 11        | > 420 m   | $\infty$    | 1260        | 2.3                      | 10                | 0.6 |

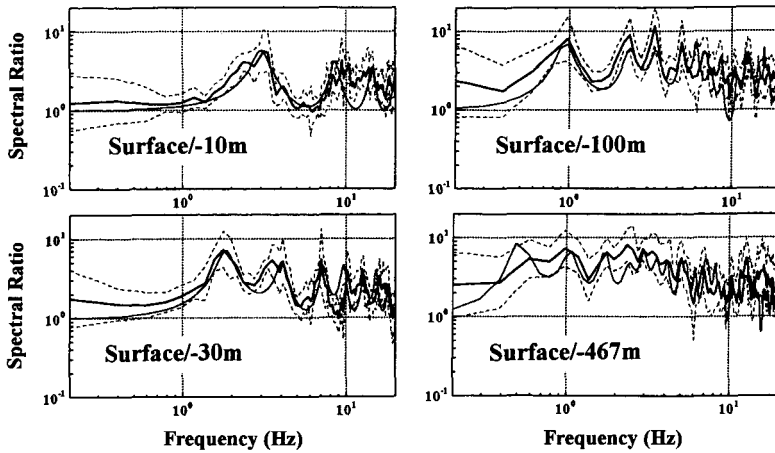


Fig. 10. Comparison between the observed spectral ratios (bold lines with dashed lines as their standard deviations) and estimated theoretical transfer functions (thin lines) at different depth levels.

good. The resulting  $Q_s$  values are quite small and have strong frequency dependency:  $Q_s = 2f^{0.7}$  for the upper most layer from surface to depth  $-11$  m.  $Q_0$  is less than or equal to 10 and  $n$  is  $0.6 \sim 0.9$  for the lower layers.

## 6. Discussion and Conclusions

The result of the PGA study shows the near-surface amplification of a factor of 2-3 for vertical component and a factor of 3-4 for horizontal components. Here we should note that the PGA amplification is not always related to S-wave amplification; in some cases, later phases (basin surface waves) have much larger amplitude than S-waves (see Fig. 3). In this sense, the PGA study is merely engineering purpose.

We estimated the  $Q_s$  values of sedimentary layers based on S-wave spectral ratios. The  $Q_s$  values are low for near surface layers, but show strong frequency dependence. There are the same results as those obtained by Takemura et al. (1993) and Saito et al. (1995) in Japan. On the other hand, Gibbs et al. (1994) obtained the constant  $Q_s$  value ( $\sim 10$ ) in California. The difference of frequency dependence of  $Q_s$  values may indicate different soil properties between Japan and California.

As shown in Fig. 3, seismograms in the Ashigara valley have large amplitude later phases that are considered to be basin surface waves. This strong

excitation of basin surface waves indicates that the total seismic response of the Ashigara valley can not be evaluated by one-dimensional method; we have to take into account the two- or three-dimensional effects. When we make two- or three-dimensional seismic response, the results of this study provide useful information about soil properties.

### Acknowledgements

This study was done as the individual study of one of the authors (Y.Y.) during one year's training course at International Institute of Seismology and Earthquake Engineering (IISEE), Building Research Institute, Tsukuba. One of the authors (Y.Y.) would like to express his deep thanks to the staffs of IISEE/BRI and JICA as well as Division of Earth and Planetary Sciences, Hokkaido University for their kindness. We especially thank Dr. K. Kudo of Earthquake Research Institute, the University of Tokyo, who kindly provided us with borehole data used in this study.

### References

- Abercrombie, R.E., 1997. Near-Surface Attenuation and Site Effect from Comparison of Surface and Deep Borehole Recordings, *Bull. Seism. Soc. Am.* **87**, 731-744.
- Celebi, M., J. Prince, C. Dietal, M. Onate, and G. Chavez, 1987. The Culprit in Mexico City —Amplification of Motion, *Earthquake Spectra* **3**, 315-328.
- Field, E.H., K.H. Jacob, and S.H. Hough, 1992. Earthquake Site Response Estimation: A Weak-Motion Case Study, *Bull. Seism. Soc. Am.* **82**, 2283-2307.
- Gibbs, J.F., D.M. Boore, W.B. Joyner, and T.E. Fumal, 1994. The Attenuation of Seismic Shear Waves in Quaternary Alluvium in Santa Clara Valley, California, *Bull. Seism. Soc. Am.*, **84**, 76-90.
- Hauksson, E., T.L. Teng, and T.L. Henyey, 1977. Results from a 1500 m Deep, Three-level Downhole Seismometer Array: Site Response, Low Q Values and  $f_{max}$ , *Bull. Seism. Soc. Am.* **77**, 1883-1904.
- Kawase, H. and T. Sato, 1992. Simulation analysis of strong motions in the Ashigara Valley considering one- and two-dimensional geological structures, *J. Phys. Earth*, **40**, 27-56.
- Kudo, K., E. Shima and M. Sakaue, 1988. Digital Strong Motion Accelerograph Array in the Ashigara Valley Seismological and Engineering Prospects of Strong Motion Observation, *Proc. 9th World Conf. Earthq. Eng.*, 119-124.
- Saito, S., T. Sasatani, and K. Kudo, 1995. Attenuation Characteristics of S Waves in the Sedimentary Layers at the Ashigara Valley, *Geophysical Bull. Hokkaido Univ.*, **58**, 39-61. (in Japanese with English illustrations and abstract)
- Sasatani, T., S. Saito, M. Furumura, and K. Kudo, 1995. The Seismic Response of the Ashigara Valley during Near-by Intermediate-depth Earthquakes, *Geophysical Bull. Hokkaido Univ.*, **58**, 21-37. (in Japanese with English illustrations and abstract)
- Schnabel, P.B., J. Lysmer, and H.B. Seed, 1972. SHAKE/A Computer Program for Earthquake Response Analysis of Horizontally Layered Sites, EERC. University of California.

Report No. EERC 72-12, Pp. 1-10

Takemura, M., T. Ikeura, K. Takahashi, H. Ishida, and Y. Ohshima, 1993. Attenuation Characteristics of Seismic Waves in Sedimentary Layers and Strong Motion Estimation," *Journal of Struct. Constr. Eng, AIJ*, **446**, 1-11. (in Japanese with English illustrations and abstract)